

2008

Mathematical Model of a Water-Water Refrigerating System

Antonio Augusto Torres Maia
Federal University of Minas Gerais

Luiz Machado
Federal University of Minas Gerais

Ricardo Nicolau Nassar Koury
Federal University of Minas Gerais

Follow this and additional works at: <http://docs.lib.purdue.edu/iracc>

Maia, Antonio Augusto Torres; Machado, Luiz; and Koury, Ricardo Nicolau Nassar, "Mathematical Model of a Water-Water Refrigerating System" (2008). *International Refrigeration and Air Conditioning Conference*. Paper 995.
<http://docs.lib.purdue.edu/iracc/995>

This document has been made available through Purdue e-Pubs, a service of the Purdue University Libraries. Please contact epubs@purdue.edu for additional information.

Complete proceedings may be acquired in print and on CD-ROM directly from the Ray W. Herrick Laboratories at <https://engineering.purdue.edu/Herrick/Events/orderlit.html>

Mathematical Model of a Water-Water Refrigerating System

Antônio A. T. MAIA^{1*}, Luiz MACHADO¹, Ricardo N. N. KOURY¹

¹Federal University Of Minas Gerais, Mechanical Engineering Department,
Belo Horizonte, Minas Gerais, Brazil
Phone: + (55 31) 3409 6667, Fax: + (55 31) 3443 3783, e-mail: aamaia@ufmg.br

ABSTRACT

The experimental study in the refrigeration field is a difficult task. In addition to the costs that are generally high and the difficulties related with the test bench construction, the experimental tests normally requires a long time and hard work to be completed. An alternative to the experimental approach consists in simulate the physical system using mathematical models. By using mathematical models the necessity of experimental data can be reduced to just the amount needed to validate the model. In this work is presented a white box mathematical model for a concentric tube evaporator of a refrigeration system. The model was validated with experimental data in steady state and transient operation. The results indicate that the model can be used as a tool in the design of refrigeration systems.

1. INTRODUCTION

In the last decades several works in the refrigeration field were developed assisted by mathematical models. The study of refrigerating fluids non aggressive to the ozone layer (Domanski et al., 1992 and Sami et al., 1995) and the development of refrigerating machines with improved energetic efficiency (Conde et al., 1991; Sand et al., 1994; Bansal et al., 1999; Tian et al., 2004; Wu et al., 2005; Maia, 2005; Liu et al., 2007; Koury et al., 2007) are some examples of mathematical models applications. In both cases, the experimental approach could require the replacement of many parts of the refrigeration system. Using a mathematical model many situations can be simulated demanding for it just the characteristics of the modified parts, which could be provided to the computational program through a data file. Even if exists a test bench available, the theoretical results can be useful if used to plan the experimental tests and to indicate the modifications that should be done in the experimental apparatus. This procedure can eliminate the less promising alternatives in advance and reduce significantly the number of experiments needed in a research work.

The purpose of this work was to develop a mathematical model to simulate the dynamic behavior of a concentric tubes evaporator. This model was based on the prototype project and built in the Mechanical Department of the Federal University of Minas Gerais.

2. EXPERIMENTAL APPARATUS

The experimental device (Figure 1) consists of a vapor compression refrigerating system, which has R134a as refrigeration fluid and, as secondary fluid, pure water in the evaporator and in the condenser. The system is basically composed by a reciprocating compressor, a condenser, a sub-cooler, an evaporator, three expansion valves and systems to do measurements and data acquisition. The compressor is alternative type and it has a piston displacement of 157 cm³. A three-phase electrical motor is employed to drive the compressor. This electrical motor is powered by a frequency inverter that enables the variation of the revolution speed of the motor-compressor assemblage in a range of 0 to 300 Hz. The condenser is shell and tube type and it has a 6 kW capacity. The secondary fluid temperature in the condenser is adjusted by mixing warm water that comes from the condenser itself with room temperature water, coming from the feeding system. The sub-cooler is coaxial type, made of an envelope tube and of an internal tube in "U". The evaporator is a multiple tube coaxial type and it is composed by a PVC envelope tube and three inner cooper tubes through which flows the refrigeration fluid. Water flows in counter flow in the space between the PVC and cooper tubes. The evaporator was designed to provide a maximum refrigeration capacity of 3 kW. In the evaporator, the secondary fluid temperature is maintained within the desired limits by an electrical heating system. The experimental bench has three expansion valves placed in parallel (manual, thermostatic and electronic type). A blockage valve permits the isolated operation of each expansion device. In this work, only a manual expansion valve was used. Eleven T-type thermocouples were implanted inside the tubes at the

where \dot{m}_{f3} , N , V , ρ_{f2} and η_v are respectively the mass flow rate, the rotational speed, the piston displacement volume, the specific mass at the compressor inlet and the volumetric efficiency. To calculate the volumetric efficiency some experimental data, shown in the Figure 1, was employed to define a correlation that relates volumetric efficiency with compressor speed, condensation temperature and evaporation temperature. This correction has the following form:

$$\eta_v = a_0 + a_1 T_{f3} + a_2 T_{f1} + a_3 N + a_4 (T_{f1})^2 + a_5 (T_{f3})^2 + a_6 T_{f3} T_{f1} + a_7 (T_{f1})^2 T_{f3} \quad (2)$$

The temperatures present in the Equation (2) are in Kelvin and the compressor speed is in revolutions per second. The values for the a_n coefficient can be found in the table 1.

Table 1 – Values for a_n coefficient

a_0	a_1	a_2	a_3	a_4	a_5	a_6	a_7
2801509.65	-14645.66	-6912.42	-1.80	13.52	18.50	21.37	-0.042

As can be seen in the Figure 1, the volumetric efficiency increases when the evaporation temperature increases, and decreases when the compressor speed is increased. The first event is related with the reduction in the relation condensing pressure/evaporation pressure. Once the condensing temperature was kept in about 45°C in all experimental tests, any augment in the evaporation temperature will contribute to reduce that pressure relation. The second event is related with the pressure losses in the compressor valves. These losses became more significant when compressor is working at higher speeds.

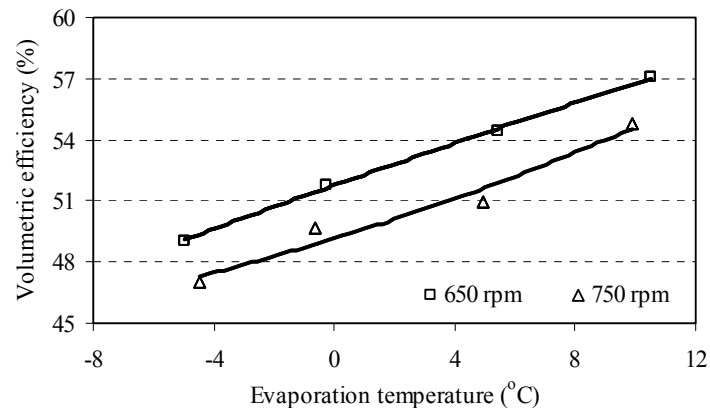


Figure 1 – Volumetric efficiency evolution regarding to evaporation temperature and compressor speed

The compressor model presented here is dependent from experimental data. This strategy was chosen because it allows developing a simple model that is able to provide good results. The experimental data needed in the compressor model development was obtained from experimental tests performed in the test bench (Figure 1), but it can also be obtained from compressor manufactures what would make this strategy even more attractive.

3.2. Evaporator model

In the evaporator model development the following simplifications were considered: (1) The refrigerant liquid and vapor phases were in thermodynamic equilibrium; (2) The axial heat transfer was neglected; (3) The evaporator has a perfect thermal insulation; (4) The physical properties related with refrigerant, secondary fluid and pipe wall were considered uniform in the evaporator cross section; (5) The refrigerant and secondary fluid potential energy was not taken into account. The input variables are the refrigerant mass inside the evaporator (M), the mass flow rate (\dot{m}_{f1}) and the refrigerant enthalpy (h_{f1}) at the inlet of the evaporator, the secondary fluid mass flow rate (\dot{m}_a), the secondary fluid temperature (t_{a1}) at the inlet of the evaporator. The output variables are the refrigerant temperature at the inlet and outlet of the evaporator, the secondary fluid temperature at the outlet of the evaporator and various spatial patterns like pressure, enthalpy and temperature. The evaporator model was established by dividing this component in to a number of control volumes and applying the principles of energy conservation (refrigerant,

secondary fluid and pipes wall), as well as mass and momentum conservation (refrigerant). This procedure generated a set of differential equations. For the refrigerant fluid (energy, mass and momentum conservation):

$$A_f \cdot \frac{\partial}{\partial t} [\rho_f \cdot (h_f - P_f \cdot v_f)] = -A_f \cdot \frac{\partial}{\partial z} (G_f \cdot h_f) + \alpha_f \cdot p_f \cdot (T_p - T_f) \quad (3)$$

$$\frac{\partial \rho_f}{\partial t} + \frac{\partial G_f}{\partial z} = 0 \quad (4)$$

$$\frac{\partial}{\partial z} \left\{ P_f + G_f^2 \cdot \left[\frac{x^2 \cdot v_v}{\alpha} + \frac{(1-x)^2 \cdot v_l}{1-\alpha} \right] \right\} = -\frac{\partial G_f}{\partial t} - \left(\frac{dP}{dz} \right)_F - g \cdot \rho_f \cdot \sin(\theta) \quad (5)$$

For the secondary fluid (energy conservation):

$$\rho_a \cdot A_a \cdot c_{pa} \cdot \frac{\partial T_a}{\partial t} = -G_a \cdot A_a \cdot c_{pa} \cdot \frac{\partial T_a}{\partial z} - \alpha_a \cdot p_a \cdot (T_a - T_p) \quad (6)$$

$$\rho_p \cdot A_p \cdot c_{pp} \cdot \frac{\partial T_p}{\partial t} = \alpha_a \cdot p_a \cdot (T_a - T_p) - \alpha_f \cdot n \cdot p_f \cdot (T_p - T_f) \quad (7)$$

The subscripts f , p , a , l and v are related with refrigerant fluid, tube wall, secondary fluid, liquid and vapor phases, respectively. The variables A , G , h , T , P , p , x , v , g , ρ , n , c and θ are the cross section area, the mass flux, the enthalpy, the temperature, the pressure, the wet perimeter, the vapor quality, the specific volume, the gravity acceleration, the specific mass, the number of tubes, the specific heat and the pipe inclination. The variable α when indexed represents the heat transfer coefficient and when it is not indexed it represents the void fraction. The mass flux can be estimated by the quotient between the mass flow rate and the cross section passage area. The refrigerant specific mass was computed using the following equation, where ρ_l and ρ_v are the liquid and vapor specific mass:

$$\rho = \rho_l + \alpha \cdot (\rho_v - \rho_l) \quad (8)$$

The correlations utilized in this work to estimate the heat transfer coefficient, the void fraction, and the pressure drop due the friction were obtained from the technical literature. To estimate the evaporation heat transfer coefficient, at first the evaporator was divided in three regions: evaporation region, liquid deficient region and superheating region. The quality (x) and the critical quality ($x_{critical}$) were used as parameters to determine the start point and the end point of each region. The critical quality was estimated using the correlation proposed by Sthapak (Maia, 2005), presented below:

$$x_{critical} = 7,943 \cdot \left[Re_v \cdot \left(2,03 \cdot 10^4 \cdot Re_v^{-0,8} \cdot (T_p - T_{sat}) - I \right) \right]^{-0,161} \quad (9)$$

where Re , T_p and T_{sat} are the Reynolds number, the wall tube temperature and the saturation temperature. Once defined the critical quality, the evaporation region was supposed to be settled while $x < x_{critical}$; the liquid deficient region was assumed to occur from $x = x_{critical}$ to $x = 1$ and the superheating region occurs when $x > 1$. For the evaporation region, the evaporation heat transfer coefficient (α_{eb}) was estimated using the correlation proposed by Dengler and Addoms (Maia, 2005). For the liquid deficient region, the heat transfer coefficient (α_{def}) was estimated using a third order polynomial as presented below.

$$\alpha_{def} = a_0 + a_1 \cdot x + a_2 \cdot x^2 + a_3 \cdot x^3 \quad (10)$$

To determine the coefficients a_i presented in the Equation (10) it is needed four mathematical relations. The first two relations can be established knowing that at the inlet and the outlet of liquid deficient region, the heat transfer

coefficient given by Equation (10) should be equivalent to the heat transfer coefficient calculated at the outlet of the evaporation region and at the inlet of the superheating region, respectively, as showed below:

$$\alpha_{def}(x_{critical}) = \alpha_{eb}(x_{critical}) = a_0 + a_1 \cdot x_{critical} + a_2 \cdot x_{critical}^2 + a_3 \cdot x_{critical}^3 \quad (11)$$

$$\alpha_{def}(1) = \alpha_v(1) = a_0 + a_1 + a_2 + a_3 \quad (12)$$

The third relation can be found knowing that $\partial \alpha_{def} / \partial z = 0$ when $x=1$:

$$\left[\frac{\partial \alpha_{def}}{\partial x} \right]_{x=1} = \left[\frac{\partial \alpha_{def}}{\partial z} \cdot \frac{\partial z}{\partial x} \right]_{x=1} = a_1 + 2 \cdot a_2 + 3 \cdot a_3 = 0 \quad (13)$$

The last relation is showed in the Equation (14). The derivatives on the left can be estimated using the last values calculated for the evaporation heat transfer coefficient (Hoffman, 1992).

$$\left[\frac{\partial \alpha_{def}}{\partial x} \right]_{x=x_{critical}} = \left[\frac{\partial \alpha_{eb}}{\partial x} \right]_{x=x_{critical}} = \left[\frac{\partial \alpha_{eb}}{\partial z} \cdot \frac{\partial z}{\partial x} \right]_{x=x_{critical}} = a_1 + 2 \cdot a_2 \cdot x_{critical} + 3 \cdot a_3 \cdot x_{critical}^2 \quad (14)$$

It was also tried to use the polynomial proposed by Wang and Toubert (1991) to estimate the heat transfer coefficient in the liquid deficient region. However, when using an inferior order polynomial approximation, it was noticed that the convergence process became worse. Better results were obtained with the Equation (10) that provided a smoother transition between each region, which improved the convergence.

For the superheating region, the heat transfer coefficient (α_s) was estimated using the correlation proposed by Dittus-Boelter. The void fraction was estimated using the correlation proposed by Hughmark. The pressure drop along the tubes for the two phase flow was compute by the Lockhart-Martinelli correlation and, for the single phase flow, it was used the correlation proposed by Fanning. Details about these correlations can be found in Maia (2005). The simultaneous solution of the Equations (3) to (7) is very complicated due the fact that the refrigerant flow and the water flow are in opposite directions. To overcome this problem the Equations (3) to (5) were solved separately using the fourth order Runge-Kutta method, along the z axis. To obtain enthalpy gradient in the z direction, the Equations (3) and (4) were combined resulting in:

$$\frac{\partial h_f}{\partial z} = \frac{1}{G_f} \left[\frac{\partial P_f}{\partial t} - \rho_f \cdot \frac{\partial h_f}{\partial t} + \frac{\alpha_f \cdot p_f}{A_f} \cdot (T_p - T_f) \right] \quad (15)$$

The mass flux gradient can be calculated by the following expression:

$$\frac{\partial G_f}{\partial z} = - \frac{\partial \rho_f}{\partial t} \quad (16)$$

To calculate the pressure gradient in the z direction it was necessary to define a modified pressure given by:

$$\bar{P}_f = P_f + G_f^2 \cdot \left[\frac{x^2 \cdot v_v}{\alpha} + \frac{(1-x)^2 \cdot v_l}{1-\alpha} \right] \quad (17)$$

From the Equation (17), the Equation (5) can be written as:

$$\frac{\partial \bar{P}_f}{\partial z} = - \frac{\partial G_f}{\partial t} - \left(\frac{dP}{dz} \right)_F + g \cdot \rho_f \cdot \sin(\theta) \quad (18)$$

The modified pressure can be determined using the Runge-Kutta method. The result obtained should be used in the Equation (17) to determine the pressure gradient in the z direction. Before applying the Runge-Kutta method in the Equation (18), the time dependent derivative was determined from the following expression:

$$\frac{\partial G_f}{\partial t} = \frac{G_f - G_f^0}{\Delta t} \quad (19)$$

where Δt is the time step and the superscript “0” refers to the values of G_f taken at $t-\Delta t$. In an analogous way, this procedure was utilized to calculate the time dependent derivatives in the Equations (15) and (16).

The solution of the Equations (6) and (7) was performed using the finite difference implicit method. In this way, the continuous physical domain was discretized and the exact derivatives were replaced by finite difference approximations. This procedure generated an algebraic finite difference approximation of the differential equations, as presented below:

$$\rho_p \cdot A_p \cdot c_{pp} \cdot \frac{T_p(i) - T_p(i)^0}{\Delta t} = \alpha_a \cdot p_a \cdot (T_a - T_p) - \alpha_f \cdot n \cdot p_f \cdot (T_p - T_f) \quad (20)$$

$$\rho_a \cdot A_a \cdot c_{pa} \cdot \frac{T_a(i) - T_a(i)^0}{\Delta t} = -G_a \cdot A_a \cdot c_{pa} \cdot \frac{T_a(j-1) - T_a(j)}{\Delta z} - \alpha_a \cdot p_a \cdot (T_a - T_p) \quad (21)$$

Where the i index refers to the center of the control volume and the j index refers to the boundary. To determine the water temperature at the outlet of each element, the following approximation was utilized:

$$T_a(j+1) = 2 \cdot T_a(i) - T_a(j) \quad (22)$$

4. MODEL VALIDATION

4.1 – Steady-state validation

To perform the steady-state model validation, the experimental data were compared with the theoretical results obtained through computer simulations. The values of the input variables as refrigerant mass flow rate, secondary fluid temperature at the inlet of the evaporator, secondary fluid mass flow rate, condensing temperature and sub-cooling temperature, etc., were obtained from experimental measurements and provided to the mathematical model through a data file. The theoretical steady-state start point was obtained using a very high step time (10^7 s). In the Figures 2 and 3 is presented a comparison between the experimental and theoretical refrigerant temperatures at the inlet and the outlet of the evaporator. At the inlet of the evaporator, the theoretical temperature showed an average deviation of 0.4°C . All of the numerical values are between the uncertainty limits of the experimental results. At the outlet of the evaporator, the theoretical temperature showed an average deviation of 1.1°C and most numerical values are between the uncertainty limits of the experimental results.

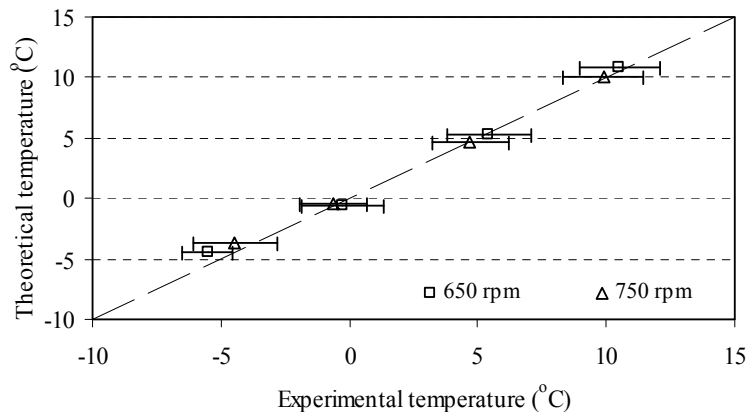


Figure 2 - Experimental and theoretical refrigerant temperature at the inlet of the evaporator

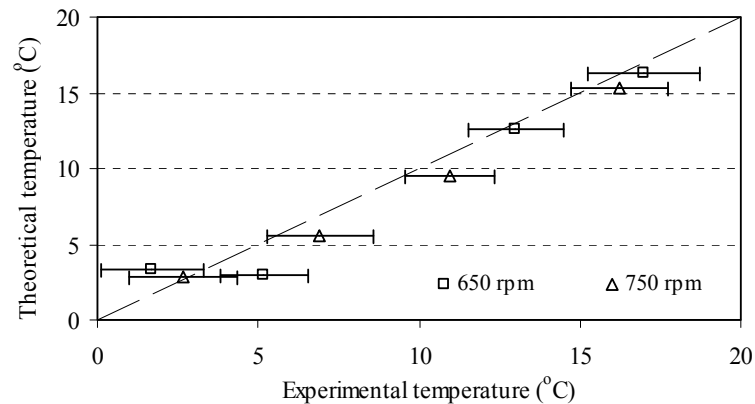


Figure 3 - Experimental and theoretical refrigerant temperature at the outlet of the evaporator

The deviations observed in the Figures 2 and 3 can be due to an inaccurate estimative of the refrigerant mass inside the evaporator. Another reason that also influenced these results is the imprecise evaluation of the heat transfer coefficient in the evaporation region. This region extends through the most part of the evaporator and its heat transfer coefficient is the higher one.

It was also carried out a comparison between the experimental and theoretical secondary fluid temperature. The agreement observed showed an average deviation of 0.2°C. This good agreement was already expected once the water temperature at the outlet of the evaporator depends basically of the refrigerating capacity and this last depends mainly to the mass flow rate, which was provided as an input variable during the process of validation.

4.2 – Transient validation

The procedure for the transient validation consisted in firstly to obtain the theoretical steady-state start point. This point was obtained using the same strategy mentioned in the steady-state validation. After this, the mass flow rate at the inlet of the evaporator was quickly reduced in 5%. The response generated by the mathematical model was compared with the experimental data obtained in an equivalent way. In the Figure 4 is presented the theoretical and experimental response to a step perturbation in the mass flow rate at the inlet of the evaporator. In this figure is being presented the refrigerant temperature at the inlet (T_{f1}) and outlet (T_{f2}) of the evaporator. These data were obtained with the evaporation temperature in approximately 10°C and compressor speed at 750 rpm. Comparing the results presented in the Figure 4 it can be noticed that theoretical data are between the uncertainty limits of the experimental results.

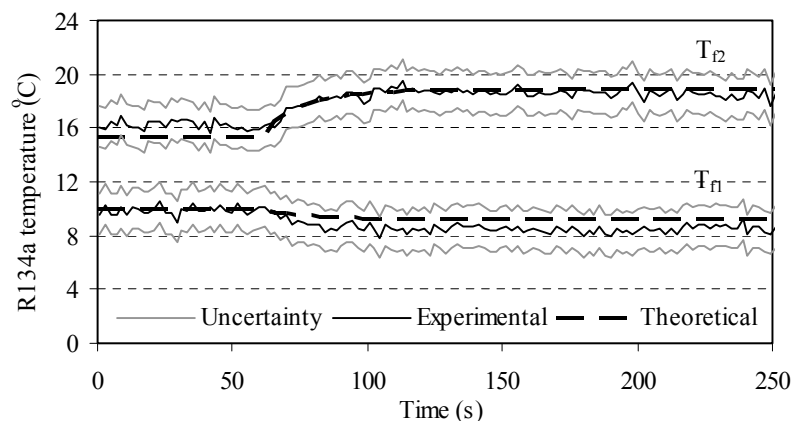


Figure 4 - Experimental and theoretical refrigerant temperature at the inlet (T_{f1}) and outlet (T_{f2}) of the evaporator

The behavior observed for T_{f1} is due to the pressure decrease at the inlet of the evaporator just after the perturbation. The response of T_{f2} is attributed to the refrigerant mass decrease inside the evaporator as a consequence of the differences between mass flow rate at the inlet and outlet of the evaporator.

6. CONCLUSIONS

In this work it was presented a mathematical model to simulate the transient behavior of a concentric tubes evaporator. The good agreement observed during the validation process showed that the proposed mathematical model and the numerical methodology utilized were effective in solving the problem. The results obtained can be improved utilizing a more accurate correlation to estimate the heat transfer coefficient in the evaporation region. The model precision can also be enhanced providing a more exact value of the refrigerant mass inside the evaporator in the start of the simulation.

REFERENCES

- Bansal, P. K. and Xie, G., 1999, A simulation model for evaporation of defrosted water in household refrigerators, *International Journal of Refrigeration*, Vol. 22, p. 319-333.
- Domanski, P. A. and McLinden, M. O., 1992, A simplified cycle simulation model for the performance rating of refrigerants and refrigerants mixtures, *Rev. Int. Froid*, Vol. 15, n° 2.
- Sami, S. M. and Zhou, Y., 1995, Numerical prediction of heat pump dynamic behavior using ternary non-azeotropic refrigerant mixtures, *International Journal of Energy Research*, Vol. 19, pp. 19-35.
- Sand, J. R., Vineyard, P. E. and Bohman, R. H., 1994, Investigation of design options for improving the energy efficiency of conventionally designed refrigerator-freezers, *ASHRAE Transac.*, v. 100, part 1, pp.1359-1368.
- Tian, C., Dou, C., Yang, X. and Li, X. , 2004, A mathematical model of variable displacement wobble plate compressor for automotive air conditioning system, *Applied Thermal Engineering*, v. 24, pp. 2467-2486.
- Wang, H. e Toubert, S Distributed and non-steady-state modeling of an air cooler. *International Journal of Refrigeration*, v. 14, p. 98-111, 1991.
- Wu, C., Xingxi, Z. and Shiming, D., 2005, Development of control method and dynamic model for multi-evaporator air conditioners (MEAC), *Energy Conversion & Management*, v. 46, pp. 451-465.
- Maia, Antônio A. T., 2005, Metodologia de desenvolvimento de um algoritmo para controle simultâneo da capacidade de refrigeração e do grau de superaquecimento de um sistema de refrigeração, Tese (Doutorado), Departamento de Engenharia Mecânica, Universidade Federal de Minas Gerais, Belo Horizonte, 160 pp.
- Conde, M. R. and Suter, P., 1991, A computer program for simulation of domestic heat pumps, *XVIII Cong. Int. Refrig.*, Montreal, pp. 1448-1453.
- Koury, R.; Maia, G., Castro, L., Machado, L., 2007, Numerical Model and Experimental Study of a Low Cost Heat Pump for Residential Water Heating, *International Congress of Refrigeration*, Beijing, China.
- Liu, Y., Wu, H., Jiang, S., Xing, Z., Shu, P., 2007, The Development of a New Generation of Open-Type Screw compressor Based on Mathematical Modeling and Experimental Investigation, *International Congress of Refrigeration*, Beijing, China.
- Hoffman, J. D., 1992, Numerical Methods for engineers and scientists, 1^a ed, USA, McGraw-Hill.

ACKNOWLEDGEMENT

The authors wish to thank FAPEMIG for the financial support.